ORIGINAL CONTRIBUTION

Enhanced solubilization of reactive dyes using mixed micellar media: insights from spectral and conductometric measurements

Fiza Bukhtawar[1] · Muhammad Usman[1] · Nadia Akram[1] · Atta ul Haq[1] · Zahoor Ahmad[2] · Saleem Raza[1] · Sadia Younis[1] · Muhammad Faizan Nazar[3]

Abstract

Surfactant molecules possess unique properties that function as a powerful solvent, removing organic contaminants from industrial effluents. It also contains hydrophilic and hydrophobic groups. In the present study, the role of a nonionic surfactant such as Triton X-100 (TX-100) is discussed in dissolving cationic micellar media of Cetyl trimethyl ammonium bromide (CTAB) for reactive dyes such as Reactive Blue-194 (RB-194) and Reactive Blue-250 (RB-250). Through UV/visible spectroscopy and electrical conductivity, we have explored various features. The values of partition coefficient K_x and change in Gibbs free energy of partition (ΔG_p) decide the suitable composition of surfactant solution with the highest solubilizing power. The parameters have been determined from UV/Visible spectroscopy data, while thermodynamic parameters (ΔG_m, ΔH_m, ΔS_m) have been calculated from specific conductivity data. The final results revealed that TX-100 has significantly enhanced the solubilization capacity of CTAB. On the other hand, the structural features of RB-250, such as smaller molecular sizes, less aromaticity, less hydrophobicity, and a lower degree of delocalization, make it more solubilized compared to RB-194.

Keywords Mixed micellar media · Micellization · Solubilization · Partition coefficient · Binding constant

Introduction

Nowadays, the research community has shown more attention to using mixed micellar media to improve the solubility of poorly water-soluble compounds and remove dissolved contaminants from aqueous systems. Surfactants are characterized by their amphiphilicity, which means they contain both polar (hydrophilic) and nonpolar (hydrophobic) components. In water, they form micelles at a critical concentration (CMC). Their properties (reducing interfacial tension and increasing wetting ability) have led to their use in many places around the house and at work. Additionally, surfactants are used a lot in the mining, printing, and textile industries [1–6].

Detergency and textile dyeing require understanding the theory and applications of solubilization. Nonionic and cationic dispersing agents were used to formulate an optimum surfactant composition with improved dye solubilizing capability. Surfactants alter dye spectra primarily by changing the surfactant's nature [7].

A further observation on the subject of mixing a nonionic surfactant with a micellar cationic solution has been noted, which substantially affects the physio-chemical properties and the solubility of the solution. Adding a cationic-to-anionic surfactant head-screening analyte usually triggers micellar transitioning from spherical to rod-like. While $C_{16}TAB$ and $C_{16}PC$ are identical in hydrophobic length, their solubilizing efficiency differs significantly. London dispersion forces and Coulombic forces influence solubility in micellar systems. $C_{16}PC$ and $C_{16}TAB$ micellization appear to be both an enthalpy and an entropy-driven process. Compared to nonionic micellar solutions alone, combined cationic and nonionic micellar solutions could provide

✉ Muhammad Usman
  musman@gcuf.edu.pk

  Fiza Bukhtawar
  fiza.bukhtawar3411@gmail.com

[1] Department of Chemistry, Government College University, Faisalabad 38000, Pakistan

[2] Department of Chemistry, University of Engineering and Technology, Lahore 54890, Pakistan

[3] Department of Chemistry, University of Education Lahore, Multan Campus, Lahore 60700, Pakistan

outstanding solubilization and detergent effects. This method may help to minimize the number of waste dyes and surfactants in textile wastewater [8, 9].

Irfan et al. studied the thermal and spectral analysis associations combining reactive anionic dyes (reactive orange 122 and red 223) and CTAB micellar environment (cationic surfactant). The experimental results demonstrate that pure CTAB has a CMC value of 1 mM. CMC of CTAB is raised by reactive orange 122 due to its structure-breaking effect. On the other hand, RR223 has a less rigid structure; as a result, it can be assimilated easily into micelles, thereby reducing ionic repulsion, improving micellization, and reducing the CMC value of the surfactant. Furthermore, the spectral data show that the dyes and surfactants have a significant dissolution rate. On the other hand, the negative sign of Gibbs free energies of partitioning and binding (ΔG_p and ΔG_b) reveals that solubilization and binding are spontaneous [10].

The mixed micelles have diverse compositions and elastic properties. Synergistic interaction between components of mixed micelle makes them thermodynamically stable and lowers the value of CMC. The mixture of ionic and nonionic surfactants can be used to (1) change micellar shape, (2) decrease the repulsion among the ionic head groups of the surfactants, (3) reduce CMC values, and (4) increase their solubilization capacity [11, 12]. On the other hand, a mixed micellar system has a greater cloud point and is applicable within a broader salinity range and temperature [11–14].

This study reports the incorporation of Reactive blue-194 (RB-194) and Reactive blue-250 (RB-250) dyes in mixed micellar media of CTAB, a cationic surfactant, and Triton X-100, a nonionic surfactant by UV/Visible spectroscopic analysis The basic molecular structures of the chemical substances used in this study are given in Table S1 (in the Supplementary information). In the present work, we have determined the solubilizing power of micellar solution of CTAB, in terms of partition coefficient and binding constant, in the absence of TX-100. Subsequently, the same experiments were performed at different concentrations of TX-100, namely: 0.09, 0.13, 0.15 and 0.17 mM. It has been observed that solubilizing power of CTAB micelles increases with the concentration of TX-100. It is expected that the present study's results will help choose the appropriate micellar media for removing pollutants from aqueous systems.

Parameters calculated

Spectroscopic parameters

Benesi-Hildebrand equation (BHE) is considered to be successful for the measurement of binding constant in the case of dye-based micelle (DM) binding [15].

$$\frac{dC_d}{\Delta A} = \frac{1}{K_b \Delta \varepsilon\, C_s^{mo}} + \frac{1}{\Delta \varepsilon} \tag{1}$$

In Eq. (1) Where

C_d = Dye concentration,

$C_s^{m0} = C_s - CMC_o$ = Analytical concentration of surfactant

ΔA = Differential absorbance (DA)

CMC_o = CMC of surfactant in absence of dye (CMC_o = 1.0 Mm for CTAB)

$\Delta \varepsilon$ = Change in absorption coefficients (Bounded and freely moving dye molecules in aqueous medium)

d = Path length (1.0 cm)

C_s = Concentration of surfactant

K_b = Binding constant

The final percentage of RB-194 and RB-250 (dyes) solubilization in the Micellar System is calculated using the Kawamura Equation (2). Its value gives information about the extent of the partitioning of dye from aqueous to micellar medium [16].

$$\frac{1}{\Delta A} = \frac{1}{K_c \Delta A_\infty \left(C_d + C_s^{mo} \right)} + \frac{1}{\Delta A_\infty} \tag{2}$$

where

ΔA = Differential absorbance

Kc = Partition constant

K_x = Partition coefficient (Dimensionless quantity)

K_x can be determined by using the Equation (3).

$$K_x = K_c \times n_w \tag{3}$$

where

n_w = No. of moles of water per liter (55.556)

In this case, the slope of the Kawamura plot can be used to calculate the value of K_c [17, 18].

It is possible to calculate change in Gibbs free energies in terms of partitioning and binding by using Equations (4) and (5) [19].

$$\Delta G_p = -RT ln K_x \tag{4}$$

$$\Delta G_b = -RT ln K_b \tag{5}$$

In the equations above where.

R = General gas constant

T = Absolute temperature

K_x = Partition Coefficient

K_b = Binding constant

Thermodynamic parameters

The graph between the electrical conductivity and the amount of surfactant gives us the CMC (Critical micelle concentration)

value. The change in the peak straight-line, also called the turning point, represents the CMC value at the critical point.

Micellization values can be calculated in terms of variations in thermodynamic quantities such as enthalpy, Gibbs free energy as well as entropy by using Equations (6), (7) and (8) [2, 20, 21].

$$\Delta \text{H}_m = -2.3(2 - \beta)RT^2 \left[\frac{\partial \left(log X_{cmc} \right)}{\partial T} \right]_P \tag{6}$$

$$\Delta \text{G}_m = (2 - \beta)RTlnX_{CMC} \tag{7}$$

$$\Delta \text{S}_m = \frac{\Delta \text{H}_m - \Delta \text{G}_m}{T} \tag{8}$$

From the equations, XCMC denotes the mole fraction that exhibits CMC and β is the degree of dissociation in terms of slopes of premicellar (PM) to post micellar regions (PMR) [19–21].

Materials and methods

Material used

The reactive blue-194 and reactive blue 250 (molar masses: 1205.38 and 1021.84 g/mol, respectively) were generously donated by Sandal dyestuff, Faisalabad, Pakistan. Surfactants such as TX-100 (extra pure grade) and CTAB (99.9% purity) were bought from Daejung, Korea and used as received. The structures of chemicals used along their specifications and resources are shown in Table 1.

Experimental methods

UV/visible spectroscopy

A series of CTAB solutions, ranging from submicellar to micellar concentration, were prepared using $3 \times 10\text{-}5$ M dye solution. A double-beam UV/visible spectrophotometer (Shimadzu UV-1700) recorded simple and differential UV/visible absorption spectra. The reference compartment obtained simple and differential absorption spectra of distilled water and dye/water binary by UV/visible spectrophotometer solutions. In contrast, an explanation of CTAB, prepared in the dye solution, was placed on the sample side [22–24].

Electrical conductivity

The electrical conductivity of a series of CTAB solutions was measured using Hanna, HI 2003–02 specific conductance meter. 0.01 M KCl solution is employed for calibration of the conductometer. In the submicellar and micellar range, the temperature was 293–323 K (with a difference of (10 K).

## Results and discussion

UV/visible spectroscopic study

Interaction of CTAB with RB-194

Figure 1a shows UV/visible absorption spectrum of aqueous solution of RB-194 in aqueous media with and without CTAB. The dye concentration was kept constant at 3×10^{-5} M. The λ_{max} of dye has been recorded to be 606 nm.

A bathochromic shift (red shift) has been observed in dye spectra in the presence of CTAB, indicating dye-surfactant association. The bathochromic shift may result from solvatochromism, a phenomenon in which dye absorption spectra shift towards higher wavelengths when solvent polarity decreases [25–29]. In this process, dye molecules get transferred from the aqueous phase (polar phase) into the micellar phase (less polar). Polar energy levels stabilize polar environments, i.e., "n" and π* molecular orbitals. The n-orbitals, i.e., nonbonding molecular orbitals, are more stable than the π* orbitals, i.e., antibonding molecular orbitals. In a less polar environment, the energy difference between n and π* decreases, facilitating n→π* transitions that occur at a higher wavelength, causing redshift [30–32]. Blue-194 has hydrophobic aromatic rings and anionic polar groups, so it should interact strongly with cationic surfactants. The spectra shift is caused by electrostatic and hydrophobic interactions between molecules of dye and CTAB [33].

The UV/visible absorbance of RB-194 increases with CTAB concentration, as evident from Fig. 1b, which indicates the large-scale incorporation of dye molecules into the micelle of CTAB. The dye's absorbance increases quickly until CMC and then decreases slowly as the dye has been accommodated in micelle to the fullest extent. However, sometimes absorbance increases slowly even after CMC because more dye molecules are incorporated into newly born micelles [34].

Electrostatic interactions were observed in the premicellar region form the Dye-surfactant ion association complex (DS).

$$D - +S^+ \rightarrow DS$$
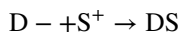
Dye-surfactant aggregates are formed as a result of the aggregation of said complexes.
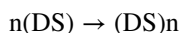
$$n(DS) \rightarrow (DS)n$$

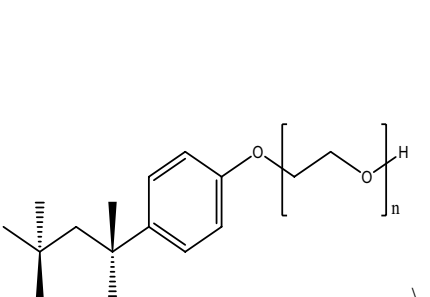**Table 1** Structures of chemicals used along their specifications and resources
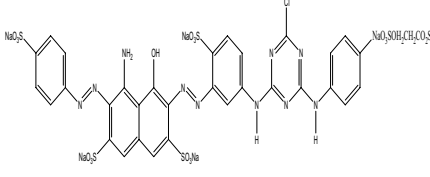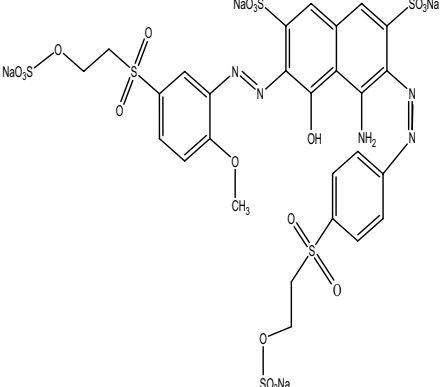
Sr. No.	Chemicals	Structure	Specifications	Resources
1	Reactive-Red (RB-194)		Molar mass: 1205.38g/mol	Sandal dyestuff, Faisalabad, Pakistan
2	Reactive Blue (RB-250)		Molar mass: 1021.84 g/mol	Sandal dyestuff, Faisalabad, Pakistan
3	CTAB		Appearance: Off-white powder Melting point:237-243C° Density: 0.5 g/cm³ Purity: 99.9%	Daejung Chemicals & metals co., LTD, Korea
4	TX-100		Appearance: Clear pale-yellow Solution Grade: Extra pure Specific Gravity at 20C°: 1.062-1.068 Melting point: 6C° Boiling Point: 270C° (at 760 mmHg)	Daejung Chemicals & metals co., LTD, Korea

Fig. 1 **a** UV/visible spectra of RB-194 in presence and absence of CTAB. **b** Plot of simple absorbance of RB-194 as a function of CTAB concentration
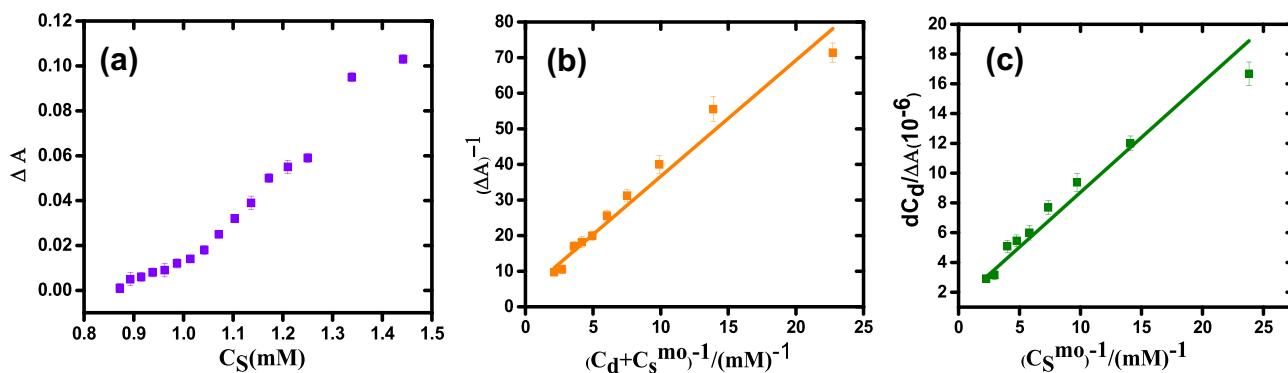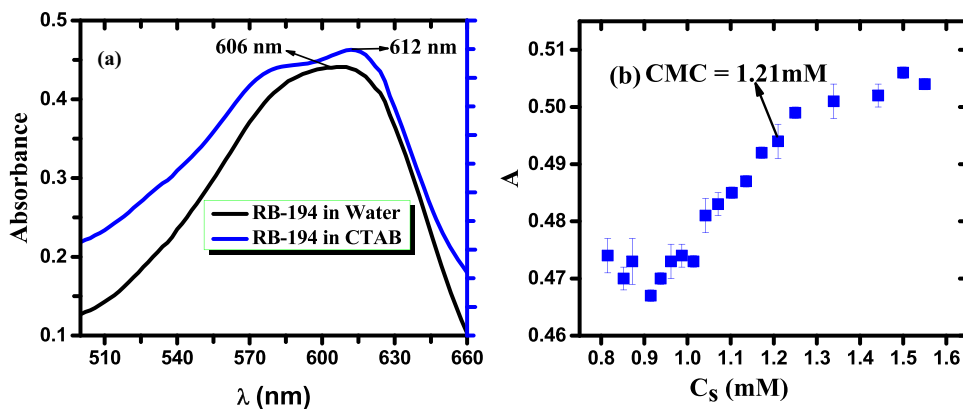

Fig. 2 **a** Plot of differential absorbance of RB-194 as a function of CTAB concentration. **b** Plot for the calculation of partition constant K_c for the RB-194/CTAB system. **c** Plot for the calculation of binding constant K_b for the RB-194/CTAB system

There is a region of the post micelles region where dye-surfactant aggregates are adsorbing onto micelles, and with time, they are solubilizing within them [35]. The differential absorbance of the said dye also increases with CTAB concentration, as shown in Fig. 2a, due to strong dye-surfactant interaction. The data of differential absorbance (shown in Table 2) has been used to calculate partition and binding parameters for RB-194/CTAB, and consequent plots are given in Fig. 2b, c.

There is a slight increase in values of differential absorbance because (1) hydrophilic and hydrophobic forces are not balancing each other, (2) solubilization is a dynamic phenomenon, and (3) micelles have a non-rigid structure [16, 36, 37]. Large K_x values, as evident from Table 3, indicate the large-scale inclusion of dye molecules into micellar media. The partitioning and binding energies have negative values (−28.54 kJ/mol and −20.10 kJ/mol, respectively), confirming the phenomena spontaneity.

Partitioning of RB-194 in mixed micellar media

Solubilization of RB-194 has been studied in the micellar solution of CTAB in the presence of 0.09 mM, 0.11 mM,

and 0.15 mM Triton X-100. It has been observed that a mixed micellar system has a more extraordinary ability to solubilize dyes. Because molecules of nonionic surfactant

Table 2 Values of differential absorbance (ΔA) with varying concentration of CTAB for RB-194/CTAB and RB-250/CTAB combined system

C_s (mM)	C_s^{mo} (mM)	$C_d + C_s^{mo}$ (mL)	Differential absorbance (ΔA)	
			RB-194	RB-250
1.44	0.44	0.47	0.103	0.113
1.33	0.33	0.36	0.095	0.096
1.25	0.25	0.28	0.059	0.087
1.21	0.21	0.24	0.055	0.081
1.17	0.17	0.20	0.050	0.074
1.13	0.13	0.16	0.039	0.073
1.10	0.10	0.13	0.032	0.068
1.07	0.07	0.10	0.025	0.064
1.04	0.04	0.07	0.018	0.056
1.01	0.01	0.04	0.014	0.050

*$CMC_o = 1.0$ mM, $C_d = 30.0$ μM

Table 3 Binding and partition constant and related Gibbs energy of for RB-194 and RB-250 in mixed micellar system (CTAB + TX-100) with varying concentration of TX-100

Combinational system	[TX-100] (mM)	$K_b \times 10^3$ (dm³mol⁻¹)	ΔG_b (kJmol⁻¹)	$K_c \times 10^3$ (dm³mol⁻¹)	$K_x \times 10^3$	ΔG_p (kJmol⁻¹)
RB-194/CTAB	0.00	3.33	−20.098	1.811	100.66	−28.54
	0.09	66.66	−27.52	44.941	2496.92	−35.88
	0.11	100	−28.52	69.865	3881.70	−37.58
	0.15	225	−30.53	148.92	8273.99	−38.80
RB-250/CTAB	0.00	8.75	−22.48	9.35	519.57	−32.6
	0.09	35	−25.92	26.23	1457.64	−35.16
	0.13	55.55	−27.06	43.73	2429.82	−36.42
	0.15	100	−28.52	109.43	6084.38	−8.7
	0.17	125	−29.07	129.42	7196.13	−39.11

get penetrated between CTAB molecules and, thus, reduce repulsive forces between ionic heads, reduce CMC, increase the size of micelle and consequently, cause enhancement in the degree of solubilization. The more negative values of ΔG_b and ΔG_p indicate that solubilization in mixed micellar solution is more spontaneous and shows a synergistic effect than in the micellar solution of individual surfactants [20, 38–40].

Interaction of CTAB with RB-250

Figure 3a shows the UV/Visible spectrum of dye with and without CTAB showing λ_{max} at 612 nm. The addition of CTAB causes a blue shift (hypsochromic shift) in the value of λ_{max} (612 to 592 nm), being a sign of dye surfactant interaction. The observed hypsochromic shift is because polar energy levels viz. n and π^* are more stabilized in aqueous media. Thus, due to the transfer of dye molecules from the

polar phase to the micellar medium, the energy gap between π and π^* increases, and the $\pi \rightarrow \pi^*$ transition occurs at a shorter wavelength and, consequently, the hypsochromic shift is observed [28].

Absorbance increases up to CMC and then acquires an almost constant value due to maximum penetration of dye molecules into micelle, as evident from Fig. 3b. Differential absorbance of RB-250/CTAB system undergoes increases with CTAB concentration, as clear from Fig. 4a, due to the inclusion of dye molecules in micelles (data of differential absorbance is shown in Table 2).

Figure 4b, c displays plots to calculate binding and partitioning parameters, respectively, and values of said parameters have been given in Table 3. The larger value of K_b (1×10^4 dm³mol⁻¹) indicates the stronger binding between CTAB and RB-250, while the larger value of K_x (6.41×10^5) suggests that migration of dye molecules from the bulk aqueous phase to micelle takes place at large scale. The value of K_x helps to predict the locus of solubilization. For RB-250,
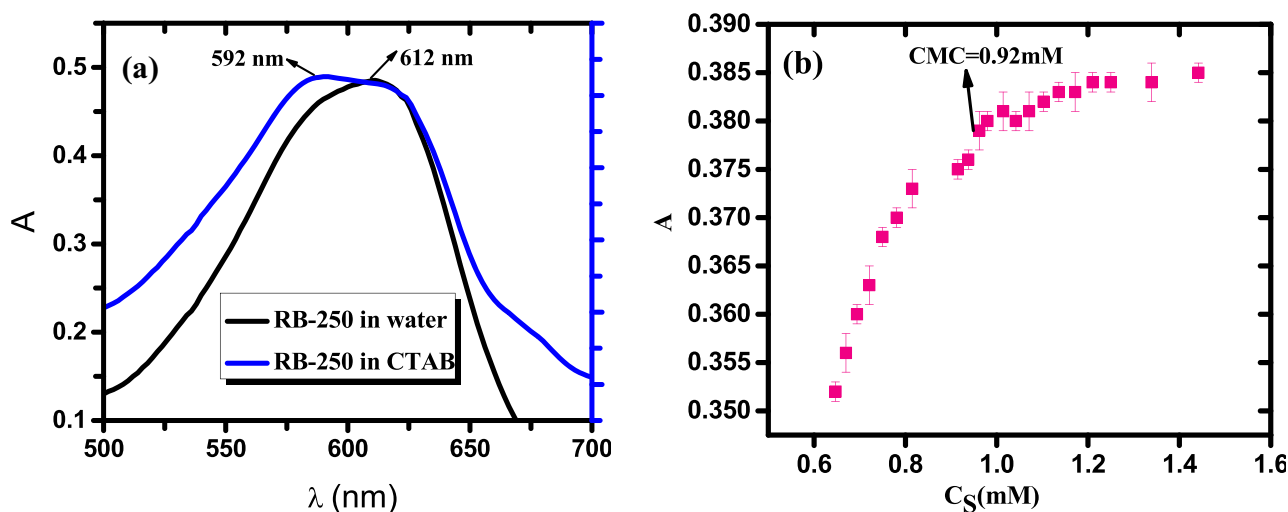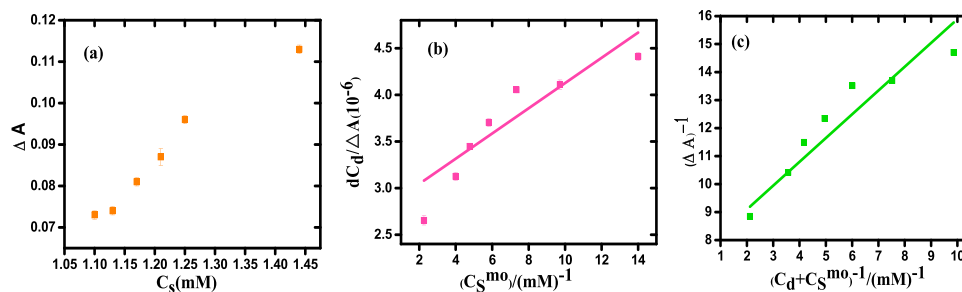

Fig. 3 **a** UV/visible spectra of RB-250 in the presence and absence of CTAB. **b** Plot of simple absorbance of RB-250 as a function of CTAB concentration

K_x is larger, indicating that its molecules reside in a micelle near the surface (in the palisade layer). In contrast, RB-194 goes relatively deeper in the micelle. However, the solubilizate does not have a fixed position in the micelle due to its dynamic nature [19].

Partitioning study of Reactive Blue-250 in mixed micellar media

In the case of RB-250 molecules in mixed micellar solutions, TX-100 showed increased solubilization in the presence of CTAB. For the said purpose, 0.09 mM, 0.13 mM, 0.15 mM, and 0.17 mM of Triton X-100 were added to the micellar solution of CTAB at a fixed concentration of dye as given in Table 3. The increasing values of binding constant (K_b), with the concentration of TX-100, indicate the stronger interactions of RB-250 in the mixed micellar system. The molecules of Triton X-100 get trapped between the cationic heads of CTAB. The result is that repulsion is minimized, and, as a result, the volume and surface area of the micelles formed is increased. The larger number of dye molecules are, thus, penetrated mixed micelles, as evident from values of K_x. The more negative values of ΔG_x and ΔG_b describe that partitioning of dye in mixed micellar media is more synergistic and spontaneous than single surfactant system [17, 41].

Comparison between interaction of RB194 and RB250 in micellar media

The molecular structures of both dyes give us a better idea of the effect of both dyes. RB-250 has greater charge density, and its lateral pressure is balanced by electrostatic attraction with cationic heads of CTAB, due to which it does not go deeper into the micelle. However, most of its molecules are solubilized in the outer portion of the micelle, where a lot of space is available. Larger values of the partition coefficient support this conclusion. While less charge density of RB194 fails to balance lateral pressure on its molecules due to which dye molecules deeply penetrate micelle due to availability of relatively narrow space and thus have lower K_x value. Thus, RB-250 is effectively removed from the aqueous solution in the presence of CTAB. The presence of small amounts of

TX-100 increases the efficiency of this micellar media. A nonionic surfactant, triton TX-100, produced micelles more effective than single surfactants at facilitating aggregation and penetration of dye molecules. Mixtures of cationic and nonionic surfactants weaken the repulsive forces between their hydrophilic heads, allowing CTAB to become more soluble by decreasing the CMC and, therefore, increasing the degree of solubilization. Furthermore, mixing a non-ionic surfactant stabilizes and enhances the hydrophobic core of the mixed micelle. The RB-250/CTAB system has a higher value of binding constants than the RB-194/CTAB system. This higher value shows stronger and more effective binding between molecules of RB-250 and CTAB. The extended conjugation and resultant large-scale delocalization in molecules of RB-194, on the other hand, reduces charge density on its anionic groups and decreases its binding affinity. It is, thus, concluded that the binding and solubilization of RB-250 is more spontaneous and takes place to a larger extent than that of RB-194.

Table 3 helps to compare the affinities of both dyes for solubilization in micellar media of CTAB. Looking at the structures of both dyes, it is clear that RB-194 is more hydrophobic and penetrates deeply into micelle where relatively narrow space is available and, thus, it has a lower value of K_x. However, a higher value of K_x has been observed for RB-250 because of being less hydrophobic. Therefore, the molecules of this dye experience more attraction for cationic heads of CTAB and get accommodated close to the micellar surface where large space is available. Micellar solution of CTAB is, thus, a more efficient medium for encapsulation of RB-250, and its efficiency increases in the presence of nonionic TX-100.

RB-250/CTAB system, in the absence of TX-100, has a higher value of binding constant, which indicates that dye molecules bind more effectively with CTAB due to less delocalization of negative charge. The extended conjugation and resultant large-scale delocalization in molecules of RB-194, on the other hand, reduce charge density on its anionic groups and decreases its binding affinity. It is concluded that the binding and solubilization of RB-250 is more spontaneous and takes place to a larger extent than that of RB-194 [20, 39–45]. The possible loci of the said dyes have been portrayed in Figs. 5 and S2.

Fig. 5 a Specific conductance versus concentration of CTAB, in presence of RB-194, at different temperatures. **b** Specific conductance versus concentration of CTAB, in presence of RB-194, at 298 K
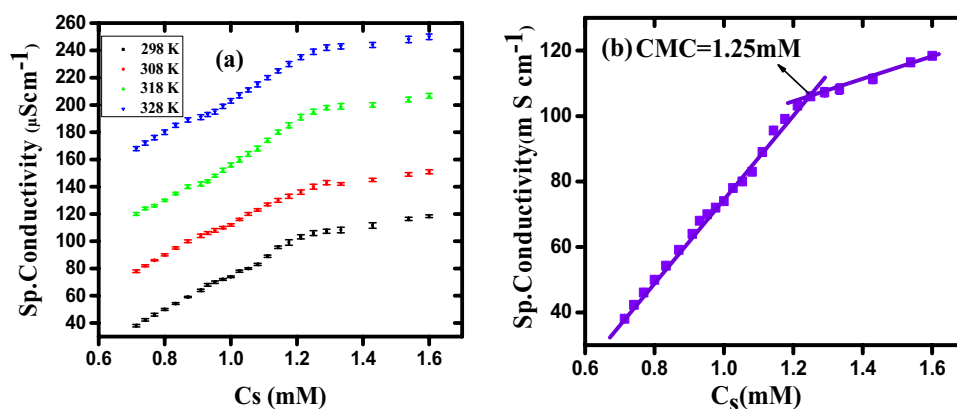
Electrical conductivity

In dilute solution (below CMC), the molecules of CTAB undergo dissociation, and there exists a dynamic equilibrium between undissociated molecules and ions produced;

$$CTAB \leftrightarrow CTA^+ + Br$$
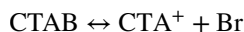
Br- ions are adsorbed at the micellar surface producing an electrical double layer with a net positive charge due to unequal distribution of charges. The Stern model explains the nature of the electrical double layer being composed of two parts (1) the Stern layer consists of strongly held counter ions and (2) a diffused layer of less strongly attached counter ions. The electrical potential decreases rapidly within the Stern layer and slowly within diffused layer [19].

Conductometric study of CTAB in the presence of reactive blue-194

The plot of the electrical conductivity of CTAB versus concentration in the presence of RB-194 is shown in Fig. 5a. Electrical conductivity gradually increases with concentration and temperature due to the increased number of free ions and their mobility. The value of CMC increases with temperature due to an increase in dehydration of hydrophobic parts of the surfactant.

Figure 5b shows how CMC was detected at 298 K. The negative values of enthalpy (ΔH_m) and Gibbs energy (ΔG_m) and positive values of entropy of micellization (ΔS_m), as evident in Table 4, show that micellization of CTAB, in the presence of RB-194, is a spontaneous, exothermic, and entropy-driven process.

The values of ΔH_m and ΔG_m become more negative with temperature because electrostatic forces become stronger with temperature rise. The negative values of ΔH_m are due to hydration of polar head groups of surfactants, and positive values of ΔS_m are due to the destruction of the water structure around hydrophobic groups [16, 19, 37, 42].

Conductometric study of CTAB in presence of Reactive blue-250

Figure 6a shows the plot of specific conductance of CTAB solution, in the presence of reactive blue 250, versus CTAB concentration.

The CMC values, at different temperatures, are measured from intersection points, as shown in Fig. 6b.

The conductivity increases with concentration; however, this increase is rapid in the sub micellar region and becomes slow after CMC due to decreased number and mobility of free ions. The temperature causes CMC to increase because of the structure breaking of water in the vicinity of hydrophobic groups. Table 4 displays the values of

Table 4 Values of thermodynamic parameters, Gibbs free energy of micellization (ΔG_m), enthalpy of micellization (ΔH_m), entropy of micellization (ΔS_m) and degree of dissociation (β) for RB-194/CTAB and RB-250/CTAB combinational system

Combinational system	T (K)	CMC (mM)	ΔG_m (kJmol^{-1})	ΔH_m (kJmol^{-1})	ΔS_m (kJK^{-1} mol^{-1})	β
RB-194/CTAB	298	1.25	−19.80	−2121964.75	−2121965	0.28
	308	1.28	−20.90	−2319483.52	−2319483	0.24
	318	1.29	−22.05	−2528738.58	−2528739	0.20
	328	1.30	−22.85	−2705225.37	−2705225	0.19
RB-250/CTAB	298	0.97	−19.82	−2.57	−2.50	0.318
	308	0.99	−21.42	−2.87	−2.80	0.238
	318	1.02	−20.96	−2.91	−2.85	0.324
	328	1.03	−21.73	−3.11	−3.05	0.316

Fig. 6 **a** Specific conductance versus concentration of CTAB, in presence of RB-250, at different temperatures. **b** Specific conductance versus concentration of CTAB, in presence of RB-250, at 298 K
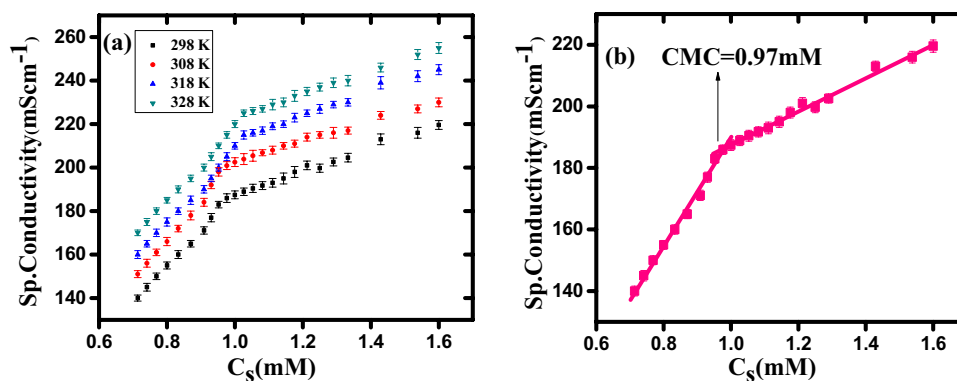
thermodynamic parameters of the CTAB/dye/water ternary system, calculated from CMC values at various temperatures. The said values favor the spontaneity and exothermic nature of micellization [19, 41].

Conclusion

Using mixed micellar media, removing organic pollutants from industrial effluents shows an excellent synergistic effect and remarkable applicability. The addition of nonionic surfactants to a micellar solution of cationic ones is not only more economical but also more efficient due to (i) increasing the aggregation number, (ii) increasing the volume/size of the micelle, (iii) reducing the CMC of the surfactant, and (iv) availability of a more hydrophobic environment [19, 46, 47]. In the light of the following points, different concentrations of a nonionic surfactant (TX-100) were mixed with a cationic surfactant (CTAB). The solubilization of reactive dyes, i.e., RB-194 and RB-250, was carried out in cationic-nonionic micelle mixed media utilizing spectroscopic and specific conductivity measurements. The higher values of binding parameters, K_x and K_b, for the RB-250/CTAB system are due to a stronger electrostatic interaction between the dye and surfactant. The RB-250 has a higher charge density due to a lower degree of charge delocalization, less hydrophobicity, and therefore becomes more solubilized. On the other hand, more hydrophobicity, higher aromaticity, and more delocalization of charges negatively influence the degree of solubility of RB-194, which leads to lower K_x values. The values of K_x predict that molecules of RB-250 will be solubilized in the outer palisade layer near the surface of the micelle, while those of RB-194 go relatively deeper. In addition, mixing TX-100 provides a synergistic effect on the solubility power of CTAB. The values of the thermodynamic parameters, i.e., ΔH_m, ΔG_m, and ΔS_m, show that solubilization is a spontaneous, exothermic, entropy-driven process. The reported study will help select suitable micellar media for environmental remediation technologies. It will also help to predict the solubility properties of mixed surfactant solutions based on those of individual surfactants [35].

Declarations

Conflict of interest The authors declare no competing interests.

References

1. Kumar D, Rub MA (2020) Alkanediyl-α, ω–type gemini micelles–catalyzed study between ninhydrin and [Ni (II)-Trp]+ complex. Colloid Polym Sci 298:1411–1421

2. Rub MA, Kumar D (2019) Interaction of ninhydrin with zinc (II) complex of tryptophan in the three dicationic gemini surfactants. Colloid Polym Sci 297:1519–1527

3. Khan AB, Bhattarai A, Jaffari ZH, Saha B, Kumar D (2021) Role of dimeric gemini surfactant system on kinetic study of alanine amino acid with ninhydrin reaction. Colloid Polym Sci 299:1285–1294

4. Bhattarai A, Rub MA, Jaffari ZH, Saha B, Thu HT, Alghamdi YG, Kumar D (2021) Spectroscopic and conductometric analyses of ninhydrin and threonine reaction in double-headed geminis. Ind Eng Chem Res 60:14977–14984

5. Rub MA, Azum N, Kumar D, Nadeem A, Khan M, Alotaibi A, Asiri AM (2021) Investigation of solution behavior of antidepressant imipramine hydrochloride drug and non-ionic surfactant mixture: experimental and theoretical study. Polymers: Polymers 13:4025

6. Rub MA, Azum N, Kumar D, Khan A, Arshad MN, Asiri AM, Alotaibi MM (2021) Aggregational behaviour of promethazine hydrochloride and TX-45 surfactant mixtures: a multi-techniques approach. J Mol Liq 342:117558

7. Muhammad MT, Khan MN (2017) Study of electrolytic effect on the interaction between anionic surfactant and methylene blue using spectrophotometric and conductivity methods. J Mol Liq 234:309–314

8. Göktürk S, Keskin G, Talman RYC, Çakır N (2017) Spectroscopic and conductometric studies on the interactions of thionine with anionic and nonionic surfactants. Color Technol 133:362–368

9. Kumar A, Kaur G, Kansal SK, Chaudhary GR, Mehta SK (2016) (Cationic+ nonionic) mixed surfactant aggregates for solubilisation of curcumin. J Chem Thermodyn 93:115–122

10. Irfan M, Usman M, Mansha A, Rasool N, Ibrahim M, Rana UA, Khan SUD (2014) Thermodynamic and spectroscopic investigation of interactions between reactive red 223 and reactive orange 122 anionic dyes and cetyltrimethyl ammonium bromide (CTAB) cationic surfactant in aqueous solution. Sci World J 540975

11. Azum N, Ruba MA, Asiria AM, Bawazeer WA (2017) Micellar and interfacial properties of amphiphilic drug–non-ionic surfactants mixed systems: surface tension, fluorescence and UV–vis studies. Colloid Surface A 522:183–192

12. Jimenez MCG, Pantoja EG, Morillo E, Undabeytia T (2015) Solubilization of herbicides by single and mixed commercial surfactants. Sc Total Environ 538:262–269

13. Burdikova J, Mravec F, Pekar M (2016) The formation of mixed micelles of sugar surfactants and phospholipids and their interactions with hyaluronan. Colloid Polym Sci 294:823–831

14. Alam MS, Ragupathy R, Mandal AB (2016) The self-association and mixed micellization of an anionic surfactant, sodium dodecyl sulfate, and a cationic surfactant, cetyltrimethylammonium bromide: conductometric, dye solubilization, and surface tension studies. J Disper Sci Technol 37:1645–1654

15. Benesi HA, Hildebrand JHJ (1949) A spectrophotometric investigation of the interaction of iodine with aromatic hydrocarbons. J Am Chem Soc 71:2703–2707

16. Kawamura H, Manabe M, Miyamoto Y, Fujita Y, Tokunaga S (1989) Partition coefficient of homologous ω-phenyl alkanols between water and sodium dodeyl sulphate micelles. J Phys Chem 93:5536–5540

17. Cheema MA, Barbosa S, Taboada P, Castro E, Siddiq M, Mosquera VA (2006) Thermodynamic study of the amphiphilic phenothiazine drug thioridazine hydrochloride in water/ethanol solvent. Chem Phys 328:243–250

18. Cheema MA, Taboada P, Barbosa S, Siddiq M, Mosquera V (2006) Effect of molecular structure on the hydration of structurally related antidepressant drugs. Mol Phys 104:3203–3212

19. Rosen MJ, Kunjappu JT (2012) Surfactants and interfacial phenomena, 4th edn. John Willey and Sons Inc, Hoboken, New Jersey, pp 150–225

20. Nazar MF, Mukhtar F, Chaudry S, Ashfaq M, Mehmood S, Asif A, Rana UA (2014) Biophysical probing of antibacterial gemifloxacin assimilated in surfactant mediated molecular assemblies. J Mol Liq 200:361–368

21. Shah SWH, Naeem K, Naseem B, Shah SS (2008) Complex formation study of hemicyanine dyes with sodium dodecyl sulfate by differential spectroscopy. Colloids Surf, A Physicochem Eng Asp 331:227–231

22. Khan A, Asim M, Usman M, Farooqi ZH, Zaman K, Rauf A, Zada A (2014) The interactions of Co-solvent, Co-solute and amphiphilic anionic dye with aqueous solutions of sodium dodecyl sulfate. Walailak J Sci Tech 12:1–13

23. Shah SWH, Naeem K, Naseem B, Shah SS (2008) Complex formation study of Hemicynine dyes with sodium dodecyl sulfate by differential spectroscopy. Colloid Surface A 331:227–231

24. Nazar MF, Mukhtar F, Ashfaq M, Rahman HMA, Zafar MN, Sumra SH (2015) Physicochemical investigation of antibacterial Moxifloxacin interacting with quaternary ammonium disinfectants. Fluid Phase Equilibr 406:47–54

25. Fazeli S, Sohrabi B, Bagha ART (2012) The study of sunset yellow anionic dye interaction with gemini and conventional cationic surfactants in aqueous solution. Dyes Pigments 95:768–775

26. Wang W, Huang G, An C et al (2017) Transport behaviors of anionic azo dyes at interface between surfactant-modified flax shives and aqueous solution: synchrotron infrared and adsorption studies. Appl Surf Sci 405:119–128

27. Hosseinzadeh R, Maleki R, Matin AA et al (2008) Spectrophotometric study of anionic azo-dye light yellow (X6G) interaction with surfactants and its micellar solubilization in cationic surfactant micelles. Spectrochim Acta A 69:1183–1187

28. Nazar MF, Murtaza S (2014) Physicochemical investigation and spectral properties of sunset yellow dye in cetyltrimethylammonium bromide micellar solution under different pH conditions. Color Technol 130:191–199

29. Nazar MF, Murtaza S, Ijaz B et al (2015) Photophysical investigations of carmoisine interacting with conventional cationic surfactants under different pH conditions. J Disper Sci Technol 36:18–27

30. Fradj AB, Lafi R, Gzara L et al (2014) Spectrophotometric study of the interaction of toluidine blue with poly (ammonium acrylate). J Mol Liq 194:110–114

31. Ali A, Uzair S, Malik NA et al (2014) Study of interaction between cationic surfactants and cresol red dye by electrical conductivity and spectroscopy methods. J Mol Liq 196:395–403

32. Khan AM, Shah SS (2008) A UV-visible study of partitioning of Pyrene in an anionic surfactant sodium dodecyl sulphate. J Disper Sci Technol 29:1401–1407

33. Nazar MF, Abid M, Danish M et al (2015) Impact of L-leucine on controlled release of ciprofloxacin through micellar catalyzed channels in aqueous medium. J Mol Liq 212:142–150

34. Rehman A, Nisa MU, Usman M, Ahmad Z, Bokhari TH, Rahman HMAU, Kiran L (2021) Application of cationic-nonionic surfactant based nanostructured dye carriers: mixed micellar solubilization. J Mol Liq 326:115345

35. Younis S, Usman M, ul Haq A, Akram N, Saeed M, Raza S, Bukhtawar F (2020) Solubilization of reactive dyes by mixed micellar system: synergistic effect of nonionic surfactant on solubilizing power of cationic surfactant. Chem Phys Lett 738:136890

36. Kumar D, Hidayathulla S, Rub MA (2018) Association behavior of a mixed system of the antidepressant drug imipramine hydrochloride and dioctyl sulfosuccinate sodium salt: effect of temperature and salt. J Mol Liq 271:254–264

37. Khan F, Rub MA, Azum N, Asiri AM (2018) Mixtures of antidepressant amphiphilic drug imipramine hydrochloride and anionic surfactant: micellar and thermodynamic investigation. J Phys Org Chem 31:e3812

38. Ayachit NH, Rani GN (2007) Excited state electric dipole moments of two exalite dyes from solvatocromic shift measurements. Phys Chem Liq 45:615–621

39. Muntaha ST, Khan MN (2020) Effect of water hardness on the interaction of cationic dye with anionic surfactants. Phys Chem Liq 58:8–17

40. Padasala S, Kanoje B, Kuperkar K et al (2016) Mixed micellization study of alkyltrimethylammonium and alkyltriphenylphosphonium bromides in aqueous solution. J Surfactants Deterg 19:389–398

41. Muntaha ST, Khan MN (2014) Study of changes in conductivity and spectral behaviour before and after micelle formation in the dye-surfactant system. J Mol Liq 197:191–196

42. Wurthner F, Kaiser TE, Saha MCR (2011) J-aggregates, from serendipitous discovery to supramolecular engineering of functional dye materials. Ange Chem Int Edit 50:3376–3410

43. Nazar MF, Raheel M, Shah SS, Danish M, Ashfaq M, Zafar MN, Siddiq M (2014) Thermodynamic characteristics and spectral luminescent properties of N-m-tolylbenzamide in microhetrogeneous surfactant selfassemblies. J Solution Chem 43:632–647

44. Nazar MF, Azeem W, Kayani A, Zubair M, John P, Mahmood A, Zafar MN (2019) pH-dependent antibiotic gatifloxacin interacting with cationic surfactant: insights from spectroscopic and chromatographic measurements. J Solution Chem 48:936–948

45. Nazar MF, Azeem W, Rana UA, Ashfaq M, Lashin A, Al-Arifi N, Mahmood A (2016) pH-dependent probing of levofloxacin assimilated in surfactant mediated assemblies: insights from photoluminescent and chromatographic measurements. J Mol Liq 220:26–32

46. Irshad S, Sultana H, Usman M, Saeed M, Akram N, Yusaf A, Rehman A (2021) Solubilization of direct dyes in single and mixed surfactant system: a comparative study. J Mol Liq 321:114201

47. Rehman A, Usman M, Bokhari TH, Rahman HMAU, Mansha A, Siddiq M, Nisa MU (2020) Effects of nonionic surfactant (TX-100) on solubilizing power of cationic surfactants (CTAB and CPC) for Direct Red 13. Colloid Surface A 586:124241